Journal of Power Sources 189 (2009) 902–908

Contents lists available at ScienceDirect

Journal of Power Sources

journal homepage: www.elsevier.com/locate/jpowsour

Improvement of the $LiBH_4$ hydrogen desorption by inclusion into mesoporous carbons

S. Cahen, J.-B. Eymery, R. Janot*, J.-M. Tarascon

Laboratoire de Réactivité et Chimie des Solides, UMR CNRS 6007, 33 rue St Leu, Université de Picardie Jules Verne, 80039 Amiens, France

ARTICLE INFO

Article history:
Received 31 October 2008
Accepted 5 January 2009
Available online 14 January 2009

Keywords:
Composites
Hydrides
Hydrogen desorption
Mesoporosity
Nanomaterials

ABSTRACT

$LiBH_4$ hydrogen desorption is strongly improved by its confinement to the nanoscale into a mesoporous carbon, prepared by the template method, having a pore diameter near 4 nm and a porous volume of 1.1 $cm^3\ g^{-1}$. The $LiBH_4$/carbon composites are prepared by room temperature impregnations of the carbon matrix with $LiBH_4$ solubilized within ethers. $LiBH_4$/carbon composites with a 33:67 weight ratio show excellent desorption kinetics with a hydrogen release of 3.4 wt.% in 90 min at 300 °C, whereas the decomposition of neat $LiBH_4$ is not significant at the same temperature. Moreover, both Differential Scanning Calorimetry and Thermal Desorption Spectroscopy experiments show that the hydrogen release for the 33:67 $LiBH_4$/carbon composite occurs in one single step immediately above the $LiBH_4$ melting temperature (280 °C) without any formation of intermediate compounds (like dodecaborane) as encountered with neat $LiBH_4$. Such modification of the hydrogen release mechanism path was never reported for confined $LiBH_4$ nanoparticles. Last the presence of the carbonaceous matrix is expected to be largely beneficial for handling the heat transfer associated with the endothermic character of the $LiBH_4$ decomposition process.

1. Introduction

Considerable attention has been recently focused on alanates and borohydrides, due to their high hydrogen contents and their possible use as hydrogen storage materials. These compounds are often called complex hydrides as they consist in a covalent group (AlH_4^- and BH_4^-, respectively) ionically bonded with alkali or alkaline-earth metals. Among them, lithium borohydride ($LiBH_4$, also named lithium tetrahydroborate) appears interesting, due to both its very high hydrogen content (18.4 wt.%) and its good volumetric capacity (121 kg m^{-3} H_2), in spite of its low crystallographic density of 0.66 g cm^{-3}. The thermal decomposition of $LiBH_4$ has been discussed in the literature [1,2]. After the $LiBH_4$ melting at approximately 280 °C, the dehydriding reaction proceeds slowly from the liquid state above 400 °C to finally lead to a solid material consisting of a mixture of boron and lithium hydride according to the following equation:

$$LiBH_4 \rightarrow LiH + B + \frac{3}{2}H_2 \quad (1)$$

The complete recovery of the whole hydrogen content of $LiBH_4$ (18.4 wt.%) remains difficult, since the thermal decomposition of LiH occurs at very high temperatures (above 600 °C) [3] limiting the hydrogen release to 13.8 wt.%. The amount of released hydrogen is nevertheless much higher than that of other families of hydrogen storage materials, but reaction (1) is highly endothermic [2] with an enthalpy of 103 kJ mol^{-1} (=69 kJ mol^{-1} H_2). Therefore, its reversibility is impossible under reasonable *P–T* conditions: the rehydrogenation of the (LiH + B) mixture has been only reported at pressure and temperature as high as 350 bar H_2 and 600 °C, respectively [4].

Several attempts have been made to increase the kinetic of hydrogen release of $LiBH_4$ by catalysts additions with the best noticeable results being obtained by ball-milling with metal oxides or chlorides [5], or mixing with SiO_2 powder [1,6]. Such additives can lower the onset temperature of dehydrogenation to about 200 °C. The other strategy for kinetic improvement that we follow in this paper is to decrease the particles size down to the nanoscale range. Owing to the shortening of the hydrogen diffusion paths, nanoparticles can promote faster absorption/desorption kinetics. In addition, the physicochemical properties (e.g. the thermodynamic) may deviate significantly from the bulk properties if the particles size is very small (usually below 2 nm), due to the large change in surface energies. Such an approach was initially put forward by Autrey and co-workers [7] for the study of the hydrogen release from ammonia borane (NH_3BH_3) incorporated into a mesoporous silica (SBA-15, pores diameter = 7.5 nm). The authors have shown that the kinetic of hydrogen release is largely improved compared to neat ammonia borane and, in addition, they have suggested that the mechanism of hydrogen desorption is modified, in spite of the relatively large particles size, as the amount of borazine $(NHBH)_3$ present in the desorbing flow is largely reduced. These results have been

* Corresponding author. Tel.: +33 3 22 82 79 01; fax: +33 3 22 82 75 90.
E-mail address: raphael.janot@u-picardie.fr (R. Janot).

0378-7753/$ – see front matter © 2009 Elsevier B.V. All rights reserved.
doi:10.1016/j.jpowsour.2009.01.002

recently further improved by using a mesoporous carbon (pores diameter in the 2–20 nm range) as the host instead of silica [8].

The preparations of $NaAlH_4$ and $LiBH_4$ nanoparticles supported on carbons have been also independently reported [9,10]. For the former, the particles were dispersed in carbon fibres through an impregnation and drying technique [9], whereas, for the latter, the hydride was directly ball-milled with mesoporous carbons [10]. In both cases, although the hydride was not really incorporated into the pores of the carbonaceous host, but rather simply deposited, a strong decrease in the onset temperature of hydrogen desorption was also found together with a much faster hydrogen release.

In the hope of avoiding particles sintering upon thermal desorption, the real inclusion of $LiBH_4$ nanoparticles into the mesopores of a carbonaceous host has been recently mentioned by Vajo and co-workers [11–13]. Mesoporous carbons called aerogels (pores diameter in the 10–40 nm range), prepared from formaldehyde and resorcinol condensation, have been impregnated with molten $LiBH_4$ at 280–300 °C. Using this process, carbon aerogels with $LiBH_4$ loadings reaching 20 wt.% have been successfully prepared. Pursuing along that line, the main objective of this paper deals with a new room temperature method for the elaboration of $LiBH_4$/carbon composites with high $LiBH_4$ contents. The hydrogen desorption mechanism of the carbon-encapsulated $LiBH_4$ nanoparticles is compared to that of bulk $LiBH_4$.

2. Experimental section

2.1. Synthesis

Commercial $LiBH_4$ powder (Acros Organics, 95%) was dissolved under stirring at room temperature in methyl tert-butyl ether (MTBE, $C_5H_{12}O$, Sigma–Aldrich, >99.8%, over molecular sieves). Solutions with a 0.1 M $LiBH_4$ concentration (217 mg $LiBH_4$ for 100 cm^3 $C_5H_{12}O$) were especially prepared, the insoluble species being removed by filtration. The mesoporous carbons were obtained by the template method according to the conditions given by Ryoo et al. [14] and Parmentier et al. [15]. Briefly, a mesoporous silica (SBA-15) was used as template and infiltrated by a solution of sucrose ($C_{12}H_{22}O_{11}$, Acros Organics, D+ saccharose). The mixture was heat-treated under vacuum at 900 °C for the conversion of sucrose to carbon. Finally, the SBA-15/carbon composite was leached with hydrofluoric acid to remove the silica matrix and recover the carbon replica. Prior to the $LiBH_4$ addition, the mesoporous carbons were dried under vacuum at 300 °C for 12 h. The impregnation of the mesoporous carbons was made by incipient wetness method with the 0.1 M solution of $LiBH_4$ in MTBE followed by drying under primary vacuum at room temperature for 12 h. Several successive steps of impregnation/drying were performed to increase the $LiBH_4$ loading of the mesoporous carbon. Except for the initial synthesis of mesoporous carbons, all experiments were carried out in a glove box filled with purified argon.

2.2. Characterizations

The samples were studied by X-ray diffraction using a Bruker D8 diffractometer (Cu Kα radiation, λ = 1.54056 Å) equipped with a position sensitive detector (PSD). Due to the reactivity with air and moisture of highly divided $LiBH_4$, an air-tightened sample holder with a beryllium window was used. This device is responsible for the presence of sharp Be/BeO reflections on the X-ray diffraction patterns. The texture/morphology of the mesoporous carbons was investigated by TEM using a Philips CM12 microscope. The powders were simply deposited on copper grids coated with a lacey carbon film. Specific surface areas and pore size/volume distribution were computed from the results of N_2 adsorption–desorption at 77 K performed with a Micromeritics ASAP 2020 analyzer. The BET (Brunauer-Emmet-Teller) and BJH (Barrett-Joyner-Halenda) formalisms were used for the calculations, respectively. The samples were outgassed under vacuum at room temperature just before the N_2 exposure. The loading in $LiBH_4$ of the carbon/$LiBH_4$ composites was deduced from the measurements of Li contents. Known weights of samples were dissolved in an acidic solution (1.0 M HCl) under vigorous stirring. Atomic absorption spectroscopy (PerkinElmer AAnalyst 300) determined the Li contents of the resulting solutions. Standard solutions of 1, 2 and 3 mg L^{-1} were initially used for the Li calibration of the spectrometer.

Calorimetric measurements were carried out by Differential Scanning Calorimetry (Netzsch DSC 204) under argon flow (100 mL min^{-1}) using sealed stainless steel crucibles with cap layers being perforated immediately before the analysis to allow hydrogen releases upon heating. A heating rate of 2 °C min^{-1} was used for all experiments. TPD experiments (temperature-programmed-desorption coupled with a mass spectrometer) were carried out on neat $LiBH_4$ and carbon/$LiBH_4$ composites with a quadripolar mass spectrometer QXK300 (VG Scientific Ltd.). The procedure consisted in loading about 5 mg of powder in a stainless steel tube (6 mm in diameter). The tube was then connected to the mass spectrometer and outgassed under a primary vacuum (10^{-2} mbar). The TPD curves were acquired at a heating rate of 10 °C min^{-1} and temperatures up to 600 °C. The hydrogen desorption was followed by volumetric measurements using a homemade Sievert-type instrument. The sample was transferred in the glove box into a stainless steel capillary that was then connected to the Sievert apparatus. After outgassing at room temperature, the hydrogen absorption/desorption properties of the sample were calculated from the pressure changes in calibrated volumes using the ideal gas law. The kinetics of hydrogen desorption were recorded using a Hiden IGA001 gravimetric analyzer equipped with an antechamber to avoid any air exposure when loading the samples. About 80 mg of material were put in a stainless steel bucket and the sample mass was continuously monitored upon desorption. Due to the $LiBH_4$ melting, a constant backup pressure of 1 bar of hydrogen (Air Liquide, purity > 99.999%) was used in order to avoid a strong bubbling of the sample and the possible squirting outside the sample bucket. The hydrogen contents, reported in the paper, are given as weight percents of the whole sample (e.g. $LiBH_4$ plus carbon).

3. Results and discussion

3.1. The mesoporous carbon

A mesoporous carbon was prepared by the template method using SBA-15 silica as matrix and sucrose as carbon precursor [14,15]. X-ray diffraction shows that the carbon exhibits an amorphous character, as a single broad peak can be detected around 26° (cf. Fig. 1a). This corresponds to a reticular distance of about 3.4 Å, which is characteristic of a poorly graphitized carbon. A hexagonal arrangement (a = 10 nm) of mesopores is easily observed by TEM (cf. Fig. 2a). The pores of the carbon replica (diameter around 4 nm) have the shape of the walls of the SBA-15 silica. The longitudinal TEM observation (cf. Fig. 2b) also reveals that the mesopores are interconnected with micropores (diameter < 2 nm) issued from the starting SBA-15 template. Therefore, a 3D porosity is present and enables the cohesion of the carbon replica. The nitrogen adsorption–desorption curve (cf. Fig. 3) of the carbon replica is a type-IV isotherm typical of a mesoporous host with a hysteresis for the relative pressures P/P_0 higher than 0.4. The BET specific surface area is equal to 1060 m^2 g^{-1} and the corresponding pore size distribution, determined from the desorption by the BJH method, is displayed as an insert. As expected from the TEM observations, a peak centred on 4 nm (mesopores) is obtained, but smaller pores

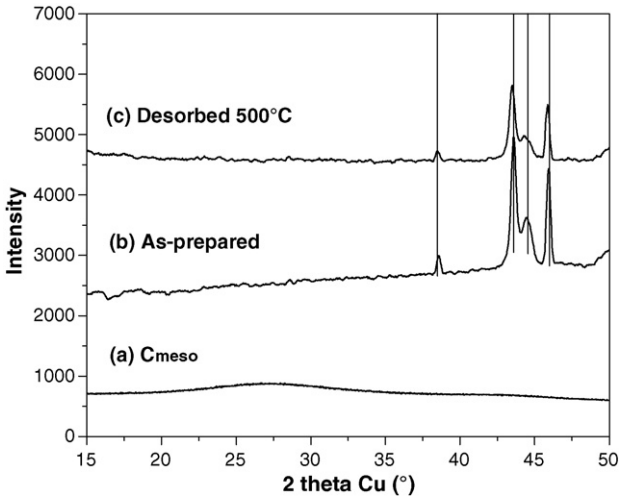

Fig. 1. X-ray diagrams of (a) the mesoporous carbon obtained by the template method, (b) the 33:67 $LiBH_4$/carbon composite and (c) the same composite after desorption at 500 °C. The reflections due to the sample holder (Be) are shown as bold lines.

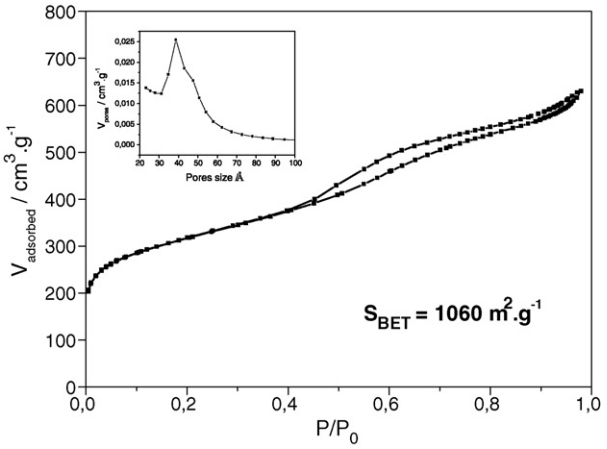

Fig. 3. Nitrogen adsorption–desorption curve at 77 K of the mesoporous carbon. Pores size distribution calculated by the BJH method is displayed as insert.

(micropores) are also present. This microporosity is highlighted by significant nitrogen adsorption for very low relative pressures (below 0.008). It is noteworthy that, in addition to the microporosity issued from the silica matrix, the sucrose process induces the formation of an additional microporosity, due to the release of volatile species during the carbonization step [15]. The porous volume (micro + meso) calculated from the value of nitrogen adsorbed at $P/P_0 = 0.95$ is 1.1 $cm^3\ g^{-1}$. As the distinctive measurement of the microporous volume cannot be achieved with nitrogen, additional experiments of CO_2 adsorption are currently being pursued. Elemental analysis conducted on this porous carbon shows its good purity. The main impurity is oxygen and its atomic content is limited to approximately 2%, a value lower than that of commercial activated carbons.

3.2. Dissolution of $LiBH_4$ in ethers

The synthesis of $LiBH_4$/carbon composites was achieved thanks to a process of liquid infiltration of the mesoporous carbon by $LiBH_4$ solutions in ethers. The X-ray diagram of commercial $LiBH_4$ is presented in Fig. 4a: all the reflections are indexable in an orthorhombic unit cell with the Pnma space group [16]. This precursor was dissolved under stirring in purified ethers at room temperature. If a large amount of $LiBH_4$ can be solvated by THF (e.g. 2.0 M solution is commercially available), the removal of the solvent remains difficult under primary vacuum, due to the formation of stable etherates, as shown on Fig. 4b where extra XRD reflections are clearly seen. These reflections are not indexed as the structures of the etherates remain unknown. Unfortunately, an additional heating to decompose these etherates can lead simultaneously to the beginning of the hydrogen desorption from $LiBH_4$ and, therefore, the recovery of pure $LiBH_4$ from THF solutions is almost impossible. To avoid the formation of such stable etherates, we dissolved $LiBH_4$ in heavier ethers, especially methyl tert-butyl ether (noted MTBE). This solvent enables the solubilization of small amounts of $LiBH_4$ with an easy recovery of pure $LiBH_4$ crystals by simple drying under vacuum at room temperature. As a matter of fact, except for the reduction in the intensity of the (200) reflection, the X-ray diagram of $LiBH_4$ previously dissolved in MTBE (cf. Fig. 4c) is rather similar to that of starting $LiBH_4$. The refined unit cell parameters ($a = 7.182$ Å, $b = 4.439$ Å, $c = 6.804$ Å) are very close to those of the initial compound and in good agreement with published values [16]. The steric effect induced by the tert-butyl group reduces the interaction between the $LiBH_4$ species and the O atoms of the ether and, thus, hinders the formation of too stable etherates. Next we are looking separately at the thermal decompositions of neat $LiBH_4$ and $LiBH_4$/carbon composites.

3.3. Thermal decomposition of neat $LiBH_4$

The DSC profile of bulk $LiBH_4$ exhibits two sharp and two broad endothermic peaks (cf. dotted curve of Fig. 5). The first sharp peak at 116 °C is related to a structural transition between the orthorhombic

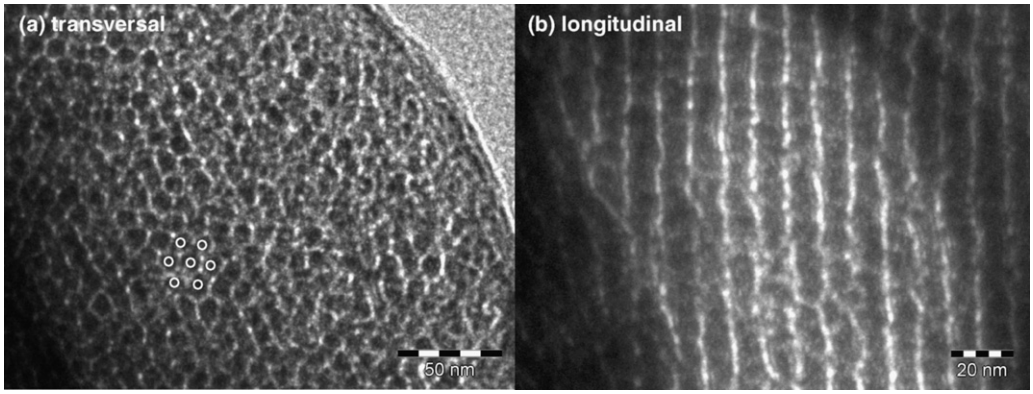

Fig. 2. TEM observations of the porous carbon obtained by the template method: (a) transversal section showing the hexagonal arrangement of mesopores and (b) longitudinal section showing the mesopores interconnected with micropores.

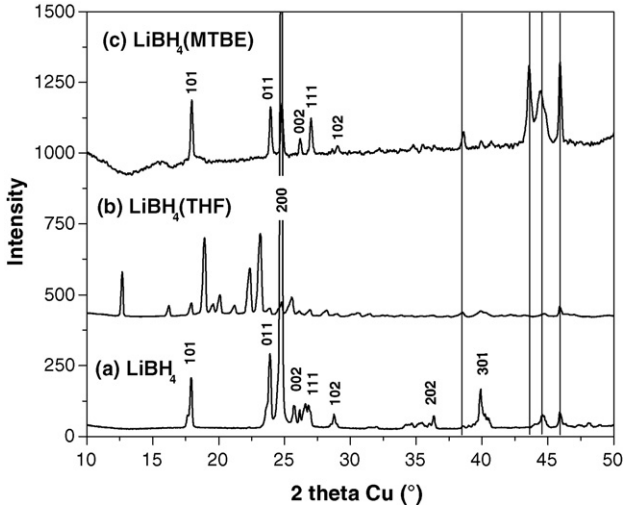

Fig. 4. X-ray diagrams of (a) commercial $LiBH_4$, (b) $LiBH_4$ previously dissolved in THF and (c) $LiBH_4$ previously dissolved in MTBE. The reflections due to the sample holder (Be) are shown as bold lines.

low temperature phase (Pnma) and the hexagonal high temperature phase ($P6_3mc$) of $LiBH_4$ [16]. The HT phase melts at 286 °C to form a liquid that desorbs hydrogen in two steps as revealed by the two broad endothermic signals at 425 and 550 °C. This two-step hydrogen desorption is well-known and the formation of "$LiBH_2$" as an intermediate compound of the desorption process was initially reported in the literature [1,2]. It is now quite well admitted that the intermediate compound is rather a mixture of LiH and lithium dodecaborane ($Li_2B_{12}H_{12}$) [17] and that the two-step desorption follows therefore the following equation:

$$LiBH_4 \rightarrow \tfrac{1}{12}Li_2B_{12}H_{12} + \tfrac{5}{6}LiH + \tfrac{13}{12}H_2 \rightarrow B + LiH + \tfrac{3}{2}H_2 \quad (2)$$

The last broad peak around 550 °C observed on the DSC curve corresponds to the formation of the final solid desorbed material (e.g. the second step of the above equation), which consists in a mixture of LiH and amorphous boron.

The enthalpies obtained for the two sharp peaks at 116 and 286 °C are 5.1 kJ mol^{-1} and 7.4 kJ mol^{-1}, in good agreement with the 4.2 and 7.6 kJ mol^{-1} values reported for the structural transition and the melting, respectively [2]. On the contrary, a value of only 54.9 kJ mol^{-1} is obtained for the enthalpy of hydrogen desorption, by taking into account the two broad peaks at 425 and

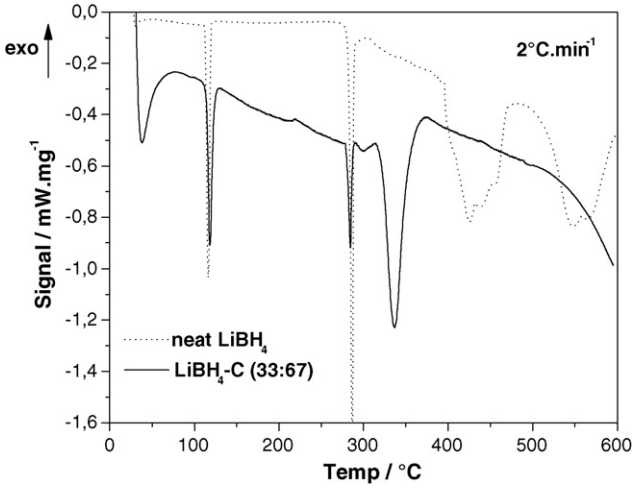

Fig. 5. DSC signals for neat $LiBH_4$ and the 33:67 $LiBH_4$/carbon composite (2 °C min^{-1}).

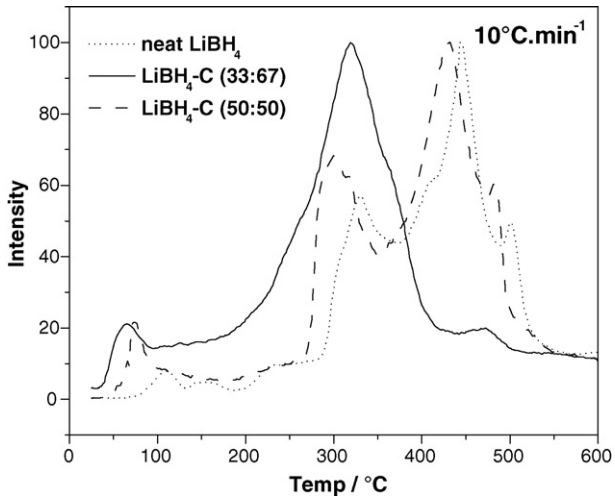

Fig. 6. TPD-MS hydrogen release curves of neat $LiBH_4$, 33:67 $LiBH_4$/carbon composite and 50:50 $LiBH_4$/carbon composite (10 °C min^{-1}).

550 °C together, which is lower than the enthalpy of 91.7 kJ mol^{-1} reported in the literature for the transformation of $LiBH_4$ (liquid) into LiH + B [2]. The origin of this discrepancy is not yet understood, but it should be recalled that great care must be taken in the enthalpies of solid–gas reactions obtained by DSC. Herein, the enthalpy of the hydrogen desorption reaction is measured under an argon flow and, therefore, the hydrogen pressure is not constant. DSC experiments under hydrogen pressure will be done in the near future to solve this issue.

In a first analysis, the thermal desorption spectra (TPD-MS) of hydrogen emission from neat $LiBH_4$ (cf. Fig. 6) displays the same four phenomena as those previously observed by DSC, meaning that each step is accompanied by the desorption of hydrogen. As a matter of fact, even the structural transition at about 110 °C leads to a small hydrogen release and, therefore, the HT phase is better written as $LiBH_{4-\varepsilon}$ [1]. After the melting of this phase at 280 °C, a significant hydrogen desorption occurs. The peak at 445 °C can be attributed to the formation of the intermediate compound ($Li_2B_{12}H_{12}$) and the hydrogen desorption is fully completed at 550 °C.

3.4. Hydrogen desorption of $LiBH_4$-impregnated mesoporous carbons

The impregnation of porous carbons by molten $LiBH_4$ at 300 °C has been recently reported [11–13]. However, in light of the aforementioned insight, one possible drawback of this process is the loss of hydrogen upon impregnation as the hydrogen desorption of $LiBH_4$ slowly occurs from the liquid state immediately above the melting temperature as observed by TPD. To avoid such a partial dehydrogenation of $LiBH_4$ and the resulting decrease in hydrogen desorption capacity of the $LiBH_4$-carbon composites, we developed in our laboratory a room temperature impregnation method of mesoporous carbons by solubilization of $LiBH_4$ in ethers. Several steps of impregnation/drying have been performed and the $LiBH_4$ contents of the resulting composites have been determined from the Li contents measured by atomic absorption spectroscopy. The properties of two different samples with $LiBH_4$/carbon weight ratios of 33:67 and 50:50 are discussed in this paper.

The BET specific surface area is drastically reduced to 16 m^2 g^{-1} by the impregnation process, regardless of the $LiBH_4$ loading content, and the mesoporous porosity is not yet observable. Thus, it seems that the carbon porosity is filled with $LiBH_4$ crystals. Fig. 1b shows the X-ray diagram of the 33:67 $LiBH_4$/carbon composite, which interestingly does not present any reflections (except those

attributed to the sample holder), due to the confinement of $LiBH_4$ to the nanoscale into the mesoporous host. The DSC profile of the same composite is shown as a bold curve in Fig. 5. The first two endothermic peaks at 118 and 284 °C correspond to the structural transition and melting of $LiBH_4$, respectively. The temperatures are almost identical to those of neat $LiBH_4$, which suggests that the thermodynamic parameters governing these two transitions are not significantly modified. One single broad endothermic peak related to hydrogen desorption is observed at 335 °C, whereas it must be recalled that the hydrogen release for neat $LiBH_4$ occurs in two steps above 400 °C. Interestingly, a quantitative analysis shows that the ratio between the areas of the hydrogen desorption peak and the melting peak (=7.4) is exactly the same as the one obtained for neat $LiBH_4$ (by cumulating the areas of the two hydrogen desorption signals for the latter). These results suggest that the overall desorption enthalpy of $LiBH_4$ is not reduced by the confinement, although an important modification appears with the absence of any formation of intermediate compounds (as $Li_2B_{12}H_{12}$) upon desorption for the composite. Finally, it is worth mentioning that no exothermic peak, which could be related to oxidation or carbide formation, is detected by DSC.

The curve of hydrogen emission recorded by TPD-MS (cf. Fig. 6) is in good agreement with the DSC results given ahead with a strong hydrogen desorption peak centred at 320 °C. At this juncture, it is important to notice that the onset temperature for hydrogen release is around 200 °C and, therefore, 100 °C lower than that of neat $LiBH_4$. Moreover, the TPD curve of the composite also displays a small hydrogen release at a very low temperature (65 °C). Its exact origin is not clear, since it cannot be attributed to the structural transition of $LiBH_4$, which still occurs around 116–118 °C after impregnation, as shown by DSC. In fact, a recent paper reports a similar feature for air-exposed $LiBH_4$ samples [18] and the authors have suggested that such a low temperature hydrogen release could be nested in the decomposition of a complex between water and $LiBH_4$. In the present study, all the composites were kept in an argon filled glove box and were not exposed to air for their characterizations. Such a complex formation with water is therefore unlikely, but cannot be totally excluded. In our opinion, the small hydrogen release at 65 °C is rather related to the decomposition of small amounts of etherates (e.g. complex between ether and $LiBH_4$), which were not completely removed upon the drying process (primary vacuum at RT for 12 h). Although such etherates formation was not observed by X-ray diffraction (cf. Fig. 4c) for neat $LiBH_4$, the presence of mesoporous carbons may perhaps favour their stability. Due to the very low particles size of $LiBH_4$ when incorporated into the porous carbon, X-ray diffraction is unfortunately unable to evidence the possible etherates. Additional characterizations using local probe techniques like IR spectroscopy and NMR, which are the most exquisite way to monitor traces of organic species, are in progress. The releases of species other than hydrogen (boranes, hydrocarbons issued from reaction with the carbonaceous host . . ..) are not detected by TPD-MS experiments. We should especially emphasize the absence of diborane (B_2H_6) release for our $LiBH_4$/carbon composites, as it is reported in the literature that B_2H_6 strongly contaminates the hydrogen desorption flow of $LiBH_4$/silica-gel mixtures [19]. This discrepancy could be explained by the different interactions between $LiBH_4$/silica and $LiBH_4$/carbon. In addition, it is worth mentioning that, in the paper of Kostka et al. [19], $LiBH_4$ is simply hand-mixed with silica-gel and, therefore, that $LiBH_4$ is not really incorporated into the mesopores.

The quantification of the hydrogen desorption for the 33:67 $LiBH_4$/carbon composite is given in Fig. 7 (squares) together with that of neat $LiBH_4$ (triangles). These data were obtained by measuring every 50 °C, from 100 to 500 °C, the amount of desorbed hydrogen using a volumetric apparatus. The calibrated volume, in which hydrogen was collected, was regularly emptied in order to always have a pressure below 1 bar. For each temperature, the measurement of the hydrogen desorption capacity was made after a total release duration of 2 h. The final hydrogen desorption capacity at 500 °C for neat $LiBH_4$ reaches 11.3 wt.%, which corresponds to 82% of the theoretical capacity (13.8 wt.% based on the formation of LiH + B). The full achievement of the desorption process for neat $LiBH_4$ requires higher temperatures and/or longer durations. The very pleasant effect provided by the $LiBH_4$ confinement to the nanoscale is the capability to release hydrogen at temperatures as low as 200 °C (cf. Fig. 7); a temperature for which neat $LiBH_4$ does not show any sign of hydrogen desorption. The total hydrogen desorption capacity at 500 °C is 4.0% per weight of composite or near 12.0% per weight of $LiBH_4$. Note that already 3.4 wt.% of hydrogen is desorbed at 300 °C for the composite, whereas only 0.2 wt.% is released for bulk $LiBH_4$ at the same temperature. Fig. 1c shows the X-ray diagram of the 33:67 $LiBH_4$/carbon composite after desorption at 500 °C. Except for the reflections due to the sample holder, no reflection is visible, which reveals that the desorbed material (LiH + B) is also embedded into the carbon mesoporosity. The carbonaceous host is therefore able to maintain the confinement of the material during the desorption process, although this one occurs mainly from the liquid state.

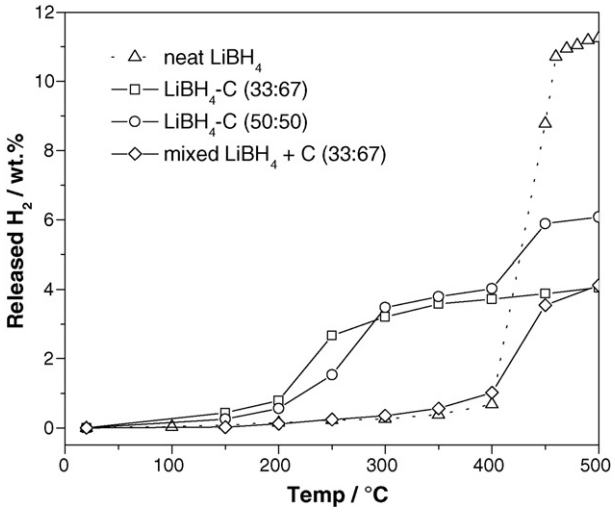

Fig. 7. Amounts of released hydrogen at different temperatures for neat $LiBH_4$, 33:67 $LiBH_4$/carbon composite, 50:50 $LiBH_4$/carbon composite and simple mixing of 33 wt.% $LiBH_4$ and 67 wt.% carbon.

Combining the results obtained with different techniques (DSC, TPD, volumetry), the positive attributes of confining $LiBH_4$ into a nanometric porosity (here 4 nm in diameter) unambiguously appear, with the most important one being the ability to start releasing hydrogen at temperatures even below the melting temperature of $LiBH_4$ (284 °C as measured by DSC). Then, hydrogen strongly evolves from the liquid state and directly leads in a single step to the final desorbed material (LiH + B), without any formation of intermediate compound, as encountered with pure $LiBH_4$. This is indicative of the feasibility to modify the hydrogen release mechanism path for a hydrogen storage material when introducing size (i.e. nanoscale) as an additional variable besides structure and composition.

To check the effect of confinement on the improvement of the hydrogen desorption performances, a sample was simply made by hand-mixing 33 wt.% of $LiBH_4$ with 67 wt.% of the same mesoporous carbon obtained by the template method. The curve of the resulting hydrogen desorption (cf. diamonds, Fig. 7) traces the one obtained for neat $LiBH_4$: the hydrogen release of the hand-made mixture does not occur below 400 °C, which confirms the strong benefit of confining $LiBH_4$ to the nanoscale range. Besides the amount of

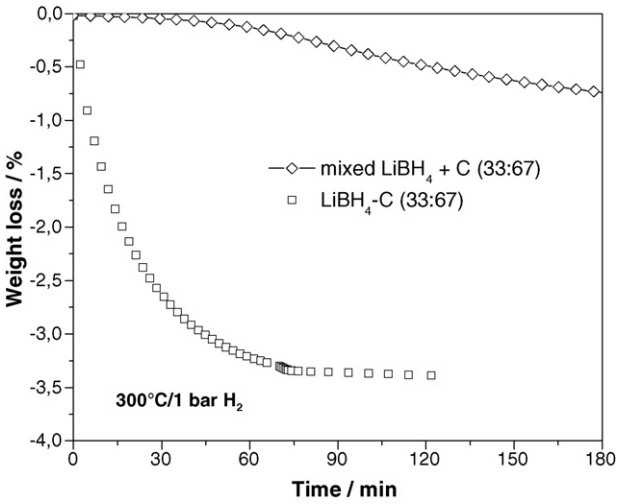

Fig. 8. Kinetics of hydrogen release at 300 °C under 1 bar H_2 for the 33:67 $LiBH_4$/carbon composite and a simple mixing of 33 wt.% $LiBH_4$ and 67 wt.% carbon.

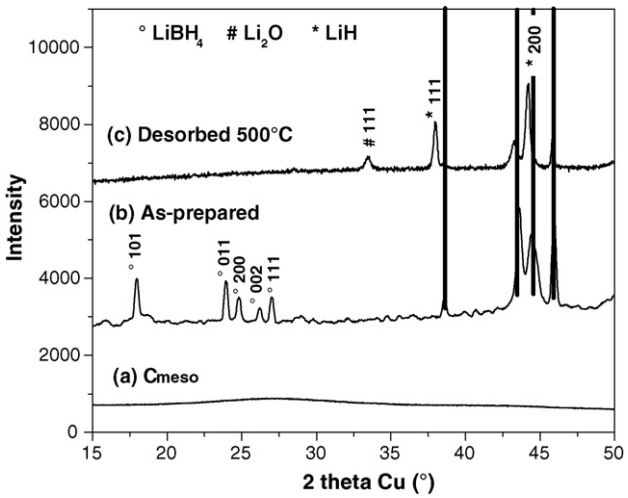

Fig. 9. X-ray diagrams of (a) the mesoporous carbon obtained by the template method, (b) the 50:50 $LiBH_4$/carbon composite and (c) the same composite after desorption at 500 °C. The reflections due to the sample holder (Be) are shown as bold lines.

desorbed hydrogen, another key parameter for applications is the hydrogen desorption kinetic. Here the kinetics were measured by the gravimetric method with a constant backup hydrogen pressure of 1 bar. The staggering enhancement of the hydrogen desorption for the 33:67 $LiBH_4$/carbon composite is nicely visualized when looking at the kinetics at 300 °C (cf. Fig. 8). For the composite, 3.4 wt.% of hydrogen is released in 90 min versus 0.3 wt.% for the hand-mixed sample. After 180 min, solely 0.7 wt.% of hydrogen is desorbed for the mixture showing the insignificant effect of carbon addition on the improvement of the $LiBH_4$ hydrogen release.

Our first attempts of rehydrogenation under 100 bar H_2 at 300 °C of the 33:67 $LiBH_4$/carbon composite were disappointing: the hydrogen absorption was barely detectable even after several hours of hydrogen exposure. Hydrogenation under higher pressures (like 350 bar as required for bulk $LiBH_4$ rehydrogenation [4]) is necessary, but we have not yet been able to conduct such experiments. This poor absorption behaviour reveals that the confinement into the carbonaceous host probably did not significantly modify the thermodynamic. The pores size (4 nm) of the mesoporous carbon is actually too large to induce a large change in surface energies and it does not allow the decrease in the large endothermic character of the desorption reaction. As a result, it appears that the synthesis of carbons with a smaller pores size is needed to the extent that liquid infiltration can proceed.

In order to increase the total hydrogen desorption capacity, we prepared composites with higher $LiBH_4$ loadings. For the sake of this paper, the performances of the highly loaded 50:50 $LiBH_4$/carbon composite are reported. Conversely to the X-ray diagram of the 33:67 $LiBH_4$/carbon composite (cf. Fig. 1b), the one corresponding to the 50:50 ratio (cf. Fig. 9b) clearly exhibits sharp reflections assigned to the low temperature phase of $LiBH_4$ (Pnma space group), suggesting that one part of $LiBH_4$ is not included in the mesopores of the carbonaceous host and remains as a bulk material onto the carbon surface. Such hypothesis was confirmed by looking at the TPD trace for the 50:50 $LiBH_4$/carbon composite (cf. Fig. 6), which looks like that of neat $LiBH_4$ with at least four hydrogen releases at about 75, 300, 430 and 480 °C. Besides the small hydrogen desorption occurring at 75 °C (which origin might be related to etherates decomposition as explained before), it should be noted that the main hydrogen release occurs through several steps above 300 °C. From the amounts of released hydrogen at different temperatures (cf. circles, Fig. 7), two domains can be described: one below 400 °C assigned to the fraction of $LiBH_4$ incorporated into the mesopores and the other one above 400 °C corresponding to $LiBH_4$ simply deposited onto the carbon surface. The total hydrogen desorption capacity at 500 °C reaches 6.0 wt.%, which is in good agreement with the 50:50 weight ratio. After desorption at 500 °C, sharp LiH reflections are observed by X-ray diffraction (cf. Fig. 9c) confirming the accomplishment of the desorption reaction. Unlikely, a concomitant oxidation also unfortunately happened as revealed by the (1 1 1) reflection of Li_2O at 33.6° (2Θ).

Among the 6.0 wt.% desorption capacity, 4.1 wt.% are desorbed at 400 °C, which is a much higher value than that of bulk $LiBH_4$ (0.6 wt.%). If we assume that this desorption capacity of 4.1 wt.% is entirely attributed to nanosized $LiBH_4$ included in the porosity of the carbon matrix, the maximum $LiBH_4$ loading of the porous carbon is 36%. Interestingly, this value comes close to the calculated amount of $LiBH_4$ (42%) that could be hosted into a carbonaceous matrix having an opened porosity of 1.1 $cm^3\,g^{-1}$ fully filled with $LiBH_4$ (crystallographic density = 0.66 g cm^{-3}). The small discrepancy with the experimental loading (36%) could be due to the difficulties in wetting the smaller pore (e.g. the micropores, $\emptyset < 2$ nm) with the etheric solutions of $LiBH_4$. Anyway, it remains that the best approach to increase the $LiBH_4$ loadings of the composites consists in the synthesis of carbon hosts with higher porous volumes.

Last, although not yet evaluated for our composites, we comment on the effect of the improvement of heat transfer, due to the carbon matrix. As a matter of fact, the hydrogen desorption reaction of $LiBH_4$ is highly endothermic (69 kJ mol^{-1} H_2) [2] and, consequently, involves a large quantity of heat. As the thermal conductivity of $LiBH_4$ is low at ambient temperature for the orthorhombic phase (around 1 W m^{-1} K^{-1} [20]), the heat transfer is poor and appears as a rate limiting step for the hydrogen release. The presence of carbon with high thermal conductivities should largely improve the heat transfer. The thermal conductivity of mesoporous carbons is generally low (even below that of $LiBH_4$ with values in the 0.1–0.5 W m^{-1} K^{-1} range for commercial activated carbons), but it is well-known that the thermal conductivity of carbons increases with their graphitization degree [21]. Conductivities as high as 180 W m^{-1} K^{-1} are reported for graphitized carbon foams [22], but such graphitized carbons have very limited porous volumes. Thus, the development of new processes for the synthesis of carbons with both a high porous volume and a significant thermal conductivity is a promising route that we are presently exploring. This finding could lead to the preparation

of new $LiBH_4$/carbon composites with high absorption/desorption performances.

4. Conclusions

In summary, $LiBH_4$/C composites were obtained by incorporating $LiBH_4$ into a mesoporous carbon ($1060\,m^2\,g^{-1}$, pores diameter = 4 nm and porous volume = $1.1\,cm^3\,g^{-1}$) prepared by the template method. The $LiBH_4$ incorporation was made through an original process of room temperature liquid impregnation using solutions of $LiBH_4$ in ethers. Such composites made of 33% by weight of nanosized $LiBH_4$ particles were shown to desorb 3.4 wt.% of hydrogen at 300 °C in 90 min, whereas neat $LiBH_4$ does not desorb at the same temperature. Moreover, we have shown using both DSC and TPD-MS techniques that the 33:67 $LiBH_4$/carbon composite can release hydrogen in one single step immediately above the melting temperature of $LiBH_4$ (280 °C). This is indicative of a strong modification of the hydrogen release mechanism path, as the hydrogen desorption process of neat $LiBH_4$ occurs above 400 °C through two different steps, due to the formation of an intermediate compound (probably $Li_2B_{12}H_{12}$). The formation of such intermediate compounds seems excluded in the case of our $LiBH_4$/carbon composites.

The overall hydrogen release for the 33:67 $LiBH_4$/carbon composite reaches 4.0 wt.% at 500 °C, which is in good agreement with the 33:67 weight ratio. We have experimentally shown that the maximum $LiBH_4$ loading of our mesoporous carbon is 36 wt.%. This value agrees well with the calculated value of 42% based on the porous volume ($1.1\,cm^3\,g^{-1}$) of carbon and the crystallographic density of $LiBH_4$ ($0.66\,g\,cm^{-3}$). Besides showing lower desorption temperatures, such composites were shown to exhibit outstanding desorption kinetics as compared to neat $LiBH_4$. With the goal of preparing new composites with still better hydrogen desorption performances, the synthesis of mesoporous carbons with both higher porous volumes and higher thermal conductivities is currently conducted; the latter aspect being critical to rapidly provide the heat needed for the hydrogen desorption reaction.

Acknowledgements

Dr. Pierre Gibot (CNRS) is gratefully acknowledged for his expertise and his help in the synthesis of the mesoporous carbons using the template method. The authors also thank Bruno Delobel (LRCS-UPJV) for the Li titrations by atomic absorption spectroscopy.

References

[1] A. Züttel, S. Rentsch, P. Fischer, P. Wenger, P. Sudan, P. Mauron, C. Emmenegger, J. Alloys Compd. 356–357 (2003) 515–520.
[2] A. Züttel, A. Borgschulte, S. Orimo, Scripta Mater. 56 (2007) 823–828.
[3] A. Zaluska, L. Zaluski, J.O. Ström-Olsen, J. Alloys Compd. 307 (2000) 157–166.
[4] S. Orimo, Y. Nakamori, G. Kitahara, K. Miwa, N. Ohba, S. Towata, A. Züttel, J. Alloys Compd. 404–406 (2005) 427–430.
[5] M. Au, A. Jurgensen, J. Phys. Chem. B 110 (2006) 7062–7067.
[6] A. Züttel, P. Wenge, S. Rentsch, P. Sudan, P. Mauron, C. Emmenegger, J. Power Sources 118 (2003) 1–7.
[7] A. Gutowska, L. Li, Y. Shin, C. Wang, X. Li, J. Linehan, R. Scott Smith, B. Kay, B. Schmid, W. Shaw, M. Gutowski, T. Autrey, Angew. Chem. Int. Ed. 44 (2005) 3578–3582.
[8] A. Feaver, S. Sepehri, P. Shamberger, A. Stowe, T. Autrey, G. Cao, J. Phys. Chem. B 111 (2007) 7469–7472.
[9] C.P. Baldé, B. Hereijgers, J. Bitter, P. De Jong, Angew. Chem. Int. Ed. 45 (2006) 3501–3503.
[10] Y. Zhang, A. Wang, L. Sun, M. Fan, H. Chu, J. Sun, T. Zhang, Int. J. Hydrogen Energy 32 (2007) 3976–3980.
[11] J. Vajo, G. Olson, Scripta Mater. 56 (2007) 829–834.
[12] J. Vajo, T. Salguero, A. Gross, S. Skeith, G. Olson, J. Alloys Compd. 446–447 (2007) 409–414.
[13] A. Gross, J. Vajo, S. Van Atta, G. Olson, J. Phys. Chem. C 112 (2008) 5651–5657.
[14] R. Ryoo, S.H. Joo, S. Jun, J. Phys. Chem. B 103 (1999) 7743–7746.
[15] J. Parmentier, S. Saadhallah, M. Reda, P. Gibot, M. Roux, L. Vidal, C. Vix-Guterl, J. Patarin, J. Phys. Chem. Solids 65 (2004) 139–146.
[16] J.P. Soulié, G. Renaudin, R. Cerny, K. Yvon, J. Alloys Compd. 346 (2002) 200–205.
[17] S. Orimo, Y. Nakamori, N. Ohba, K. Miwa, M. Aoki, S. Towata, A. Züttel, Appl. Phys. Lett. 89 (2006) 219201–219203.
[18] L. Mosegaard, B. Moller, E. Jorgensen, U. Bösenberg, M. Dornheim, J. Hanson, Y. Cerenius, G. Walker, H. Jakobsen, F. Besenbacher, T. Jensen, J. Alloys Compd. 446–447 (2007) 301–305.
[19] J. Kostka, W. Lohstroh, M. Fichtner, H. Hahn, J. Phys. Chem. C 111 (2007) 14026–14029.
[20] A.V. Talyzin, O. Andersson, B. Sundqvist, A. Kurnosov, L. Dubrovinsky, J. Solid State Chem. 180 (2007) 510–517.
[21] A. Celzard, J.F. Marêché, G. Furdin, Prog. Mater. Sci. 50 (2005) 93–179.
[22] C.N. Gallego, W.J. Klett, Carbon 41 (2003) 1461–1466.